SM Online
Scientific Resources

SM Journal of Pharmacology and Therapeutics

Research Article

Understanding the Bioavailability of Ca^{2+} in Biological Fluids in the Presence of Risedronic Acid

Bretti C[1], Cataldo S[2], Cigala RM[1], Lando G[1], Pettignano A[2] and Sammartano S[1]

[1]*Department of Chemical, Biological, Pharmaceutical and Environmental Sciences, University of Messina, Italy*

[2]*Department of Physics and Chemistry, University of Palermo, Italy*

Article Information

Received date: Nov 07, 2016
Accepted date: Dec 19, 2016
Published date: Jan 02, 2017

***Corresponding author**

Gabriele Lando, Department of Chemical, Biological, Pharmaceutical and Environmental Sciences, University of Messina, Viale Ferdinando Stagno d'Alcontres, 31, I - 98166 Messina (Vill. S. Agata), Italy, Tel: +39 090 676 5748; Email: glando@unime.it

Keywords Ca^{2+}; Bioavailability; Risedronic acid; Calorimetry; Potentiometry; Modeling; Case studies (Urine, Saliva, Human blood plasma)

Abstract

In this work, potentiometric and calorimetric measurements were carried out in aqueous NaCl solutions at different temperatures ($283.15 \leq T / K \leq 318.15$) and ionic strengths ($0 < I / mol\ dm^{-3} \leq 3.0$), to study the interaction of Ca^{2+} and Risedronic Acid (RA), a drug used for the treatment of various bone disorders and belonging to the class of Biphosphonates (BP).

The experimentally determined speciation model of the Ca^{2+}/Risedronate system consists of four species, namely the neutral CaH_2L and Ca_2L and the negatively charged $CaHL^-$ and CaL^{2-}. Calorimetric experiments allowed us to determine the thermodynamic properties of the various species, and to calculate formation constants at temperature different than 298.15 K. All the species (except the Ca_2L) resulted exothermic and the main contribution to the stability is entropic in nature.

The aim of the paper is to predict the influence of the risedronate on the speciation of Ca^{2+} in various simulated biological fluids as human blood plasma, urine and saliva.

Introduction

Risedronic acid (Figure 1) belongs to the class of Biphosphonates (BP), widely used in the medical field to treat bone disorders. Recently, it was found that risedronate may preserve bone microarchitecture in breast cancer survivors [1]. Bisphosphonates (BPs, e.g., alendronate, risedronate, and ibandronate) help to maintain bone mass, to inhibit osteoclast-mediated bone resorption, and to reduce the risk of both vertebral and non-vertebral fractures [2,3], even if atypical femoral fractures tend to occur in Asian women with prolonged bisphosphonate exposure [4]. Both alendronate and risedronate were found to be good drugs for the treatment of osteoporosis and Paget's disease, having similar effect when evaluating mineral/matrix ratio, but alendronate resulted more effective that risedronate in terms of relative proteoglycan content, mineral maturity/crystallinity and pyr/divalent collagen cross-link ratio [5]. The clinical efficacy of BPs is mainly based on two key properties: their capacity to strongly bind hydroxyapatite crystals of bone, and their inhibitory effects on osteoclast precursors and mature osteoclasts [6]. Malavasi, et al. [7] showed that risedronate can modulate positively osteoblast differentiation. In addition, authors suggest that risedronate could be considered as potential molecule to be incorporated on the surface of dental implants. Interaction of risedronate with hydoxyapatite was studied by FTIR, Raman and solid NMR spectroscopies by Errassifi, et al. [8], suggesting that risedronate adsorption on apatitic supports corresponds to an ion substitution reaction with phosphate ions at the crystal surface. The interaction of risedronate with bone mineral hydroxyapatite was studied by Mukherjee, et al. [9] and Ironside, et al. [10] with not fully aligned conclusions. Solid state interaction between alendronate and different metal cations was studied by Deacon, et al. [11]. Interaction of risedronate with metal cations is poorly investigated. Qualitatively, it is indicated that adsorption of risedronate is inhibited when the drug is taken with mineral water containing a high level of calcium or magnesium [12], but chemico-physical results are missing. A review about complexing ability of biphosphonates, not considering risedronate, was recently published by Matczak and co-workers [13] reporting that the stability of Mg^{2+} complexes is quite higher than that of Ca^{2+} homologous species, in agreement of what found by Foti, et al. [14] for etidronic acid. Recently, Bretti, et al. [15] studied the protonation sequence and the thermodynamic properties of risedronate in various media, finding that in solution the diprotonated risedronate species is a mixture of the N,P (52%) and P1,P2 (48%) tautomers.

In this work, the interaction of Ca^{2+} with risedronate is investigated by means of potentiometric and calorimetric measurements to determine the influence on the speciation of the Ca^{2+} cation in simulated human blood plasma, saliva and urine. These fluids were chosen because risedronate may be administered by means of oral tablets or intravenous injection, whereas urine is the way of excretion of this drug. Computer modeling allowed us to predict the species formed in these media, knowing all the network of interactions among all the components of the fluids, together with their analytical concentrations.

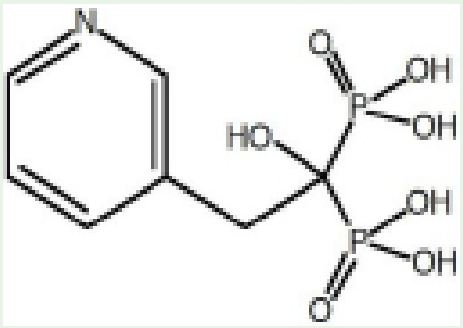

Figure 1: Chemical structure of risedronic acid.

Experimental section

Chemicals: RA solutions were prepared by weighing risedronic acid monohydrate, 99%, supplied by HEHUI CHEMICAL CO., LIMITED, P.R. China. The resultant concentrations were checked potentiometrically by alkalimetric titrations. Hydrochloric acid (HCl) and Sodium Hydroxide (NaOH) were prepared by diluting concentrated stock solutions (ampoules from Sigma Aldrich), and standardized against sodium carbonate and potassium hydrogen phthalate, respectively, previously dried in an oven at T = 383.15 ± 0.1 K for two hours. Sodium chloride was dried in an oven at T = 383.15 K for at least 2 hours, whereas $CaCl_2 \bullet 2H_2O$ aqueous solutions were standardized against EDTA standard solutions. All solutions were prepared with analytical grade water (ρ = 18 MΩ cm) using grade A glassware.

Apparatus and procedure for potentiometric measurements: Metal cation complex formation constants were determined by means of potentiometric measurements. A detailed description of the apparatuses has been reported earlier [16-18]. Instrumental errors are ± 0.15 mV and ± 0.003 cm^3 for the e.m.f. readings and titrant delivery, respectively.

For the determination of Ca^{2+}/Ris^{4-} complex species, suitable amounts of risedronic acid ($0.5 \le c_L$ / mmol $dm^{-3} \le 3.0$), $CaCl_{2(aq)}$ ($0.5 \le c_M$/mmol $dm^{-3} \le 2.5$), $HCl_{(aq)}$ and $NaCl_{(aq)}$ were added to reach pre-established values of pH (~ 2.0) and ionic strengths ($0.1 \le I$ / mol $dm^{-3} \le 3.0$) and the titrand solutions were titrated with standard base to reach pH ~ 11.0. Full experimental details are given in (Table 1).

Potentiometric measurements were performed at different temperatures, whose value was maintained constants in all the phases using water circulation from a thermocryostat (mod. D1-G Haake)

Apparatus and procedure for calorimetric measurements: Calorimetric experiments were performed using a nano-ITC low volume calorimeter (TA Instruments) equipped with a reference and sample cell (0.943 cm^3), following the recommended procedures reported by Sgarlata, et al. [19]. Measurements were run in the overfilled mode which does not require any correction for liquid evaporation and/or for the presence of the vapor phase. All titrations were carried out at T = 298.15 K using a 0.250 cm^3 syringe with a stirring rate of 300 rpm. The reference cell was always filled every day with ultra pure water (ρ = 18 MΩ cm). All solutions were degassed for 5 minutes before starting the experiments to eliminate air bubbles. For the determination of the ligand protonation enthalpy changes, the sample cell was filled with $H_4(Ris)_{(aq)}$ solution ($0.1 \le c_L$/mmol $dm^{-3} \le 10$), sodium hydroxide to neutralize desirable number of protons and the syringe filled with $CaCl_{2(aq)}$ ($0.5 \le c_M$/mmol $dm^{-3} \le 4.0$); for measurements in the presence of NaCl, this was added in equal amount both in the syringe and in the cell. For each calorimetric measurement dilution measurements (used as blank) were performed. In these runs risedronate and acid were not present in the sample cell whereas the titrant was the same of the measurement. Full eexperimental details are given in (Table 1).

Calculations: The ESAB2M program [20] was used to refine all the parameters of the acid-base potentiometric titrations (E^0, K_w, liquid junction potential coefficient, ja, and analytical concentration of reagents) whereas the BSTAC 21 software was used in the calculation of equilibrium constants. The non linear least square computer program LIANA was used to fit different equations [21]. Distribution diagrams were drawn using HySS computer program [22].

All equilibria described in this paper are expressed with the following equations:

$$jM^{n+} + H_iL^{i-4} = M_jH_iL^{(i+jn-4)} \qquad K_{ij} \qquad (1)$$

or

$$jM^{n+} + iH^+ + L^{4-} = M_jH_iL^{(i+jn-4)} \qquad \beta_{ij} \qquad (2)$$

where L is the risedronate anion (RIS^{4-}). If j = 0, eq. (2) refers to protonation constants $\left(\log K_i^H\right)$, if i < 0 and no ligand is present, eq. (2) refers to metal hydrolysis constants $\left(\log K_i^*\right)$. Throughout the paper, uncertainties are given as standard deviation. The conversion from the molar to the molal concentration scale was performed using the appropriate density values [23].

The ionic strength dependence of the equilibrium constants was studied in this work by means of the extended EDH (Extended Debye-Hückel equation) and the SIT (Specific ion Interaction Theory) [24-28] model. Considering a generic protonation constant, expressed as in eq. (2), and expressing the equilibrium constants as a function of the activity coefficients (see eq. (3)),

$$\log K_{ij} = \log K_{ij}^0 + j \cdot \log \gamma_{M^{n+}} + i \cdot \log \gamma_{H^+} + \log \gamma_{L^{4-}} - \log \gamma_{M_jH_iL} \quad (3)$$

both models are based on the assumption that the variation of the activity coefficients with ionic strength can be expressed with the general formula

$$\log \gamma = -z^2 \cdot 0.15 \cdot D.H. + f(I) \qquad (4)$$

which for the reaction described in eq. (1-2) becomes:

$$\log K_{ij} = \log K_{ij}^0 - 0.51 \cdot z^* \cdot D.H. + f(I) \qquad (5)$$

$$D.H. = \frac{\sqrt{I}}{1 + 1.5 \cdot \sqrt{I}} \qquad (5a)$$

$$z^* = \sum(\text{charge})^2_{\text{reactant}} - \sum(\text{charge})^2_{\text{Product}} \qquad (5b)$$

Where $\log K_{ij}^0$ is the equilibrium constant at infinite dilution and $f(I)$ is a term that takes into account the dependence on ionic strength. The differences between the two models regard: i) the concentration scale adopted, which is the molar one for the EDH

equation and molal one for the SIT model and ii) the nature of the term *f(I)*, that it is $f(I) = C_i \bullet I_c$ for the EDH equation and $f(I) = \Delta\varepsilon_i \bullet I_m$ for the SIT model. In turn, $\Delta\varepsilon_i$ is the combination of the specific interaction coefficients of the species involved in the equilibrium and the ions of the supporting electrolyte. For example, in the case of eq. (2) in $NaCl_{(aq)}$, it is:

$$\Delta\varepsilon_{ij} = j\cdot\varepsilon\left(M^{n+},Cl^{-}\right)+i\cdot\varepsilon\left(H^{+},Cl^{-}\right)+\varepsilon\left(Na^{+},L^{4-}\right)-\varepsilon\left(Na^{+}/Cl^{-},M_jH_jL^{(i-4)}\right) \quad (6)$$

if a neutral species is involved, eq. (4) becomes:

$$\log\gamma = k_m \cdot I \quad (7)$$

Where k_m is the Setschenow coefficient [29].

Values of the enthalpy change $\left(\Delta H_{ij}^{0}\right)$ for the metal complex formation constants were used to determine the equilibrium constantd at different temperatures according to the following equation:

$$\log K_{ij}^{T} = \log K_{ij}^{\theta} + \Delta H_{ij}^{0}\cdot F_1\left(T\right) \quad (8)$$

where

$$\Delta H_{ij}^{0} = \Delta H_{ij0}^{0} - z^{*}\cdot 1.5\cdot I^{0.5}\Big/\left(1+1.5\cdot I^{0.5}\right)+\Delta\varepsilon'_{ij}\cdot I \quad (8a)$$

$$F_1\left(T\right) = \left(1/\theta - 1/T\right)\cdot 52.23 \quad (8b)$$

θ is the reference temperature (in our case θ = 298.15 K), ΔH_{ij0}^{0} is the enthalpy change at infinite dilution, $\Delta\varepsilon'_{ij}$ is the ionic strength dependence parameter of ΔH_{ij}^{0}, z^{*} is reported in eq. (5b) and 52.23 = 1/(R·ln10) in kJ mol^{-1}.

Combining eq. (5) and eq. (8), the general equation for the analysis of the ionic strength and temperature dependence is:

$$\log K_{ij} = \log K_{ij}^{0} - z^{*}\cdot 0.51\cdot I^{0.5}\Big/\left(1+1.5\cdot I^{0.5}\right)+\Delta\varepsilon_{ij}\cdot I+\left(\Delta H_{ij0}^{0} - z^{*}\cdot 1.5\cdot I^{0.5}\Big/\left(1+1.5\cdot I^{0.5}\right)+\Delta\varepsilon'_{ij}\cdot I\right)\cdot F_1(T) \quad (9)$$

This equation is also valid for the molar concentration scale, if " $\Delta\varepsilon_{ij}$ " is substituted by C_{ij}, ΔH_{ij0}^{0} by A_T, and $\Delta\varepsilon'_{ij}$ *by* C'_{ij}.

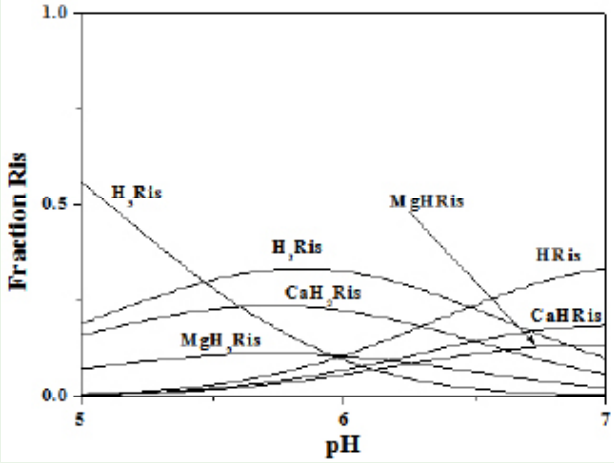

Figure 2: Speciation of risedronate in urine at *T* = 310.15 K and *I* = 0.3035 mol dm^{-3}.

Table 1: Experimental conditions adopted for potentiometric and calorimetric measurements on the Ca^{2+}/Ris^{4-} system.

Potentiometric measurements					
T / K	*I*[a]	c_H[b]	c_L[b]	c_M[b]	n.tit
283.15-310.15	0.1 to 3.0	5.0 to 10.0	0.5 to 3.0	0.5 to 2.5	45
Calorimetric measurements					
T / K	*I*[a]	Cell		Burette		n.tit
		c_H[b]	c_L[b]	c_H[b]	c_M[b]	
298.15	0.15	1.0 to 6.0	1.0 to 3.0	-	2.0 to 5.0	5

[a]mol dm^{-3}; [b]mmol dm^{-3}.

Results and Discussion

Complex formation constants and enthalpy changes

The experimental conditions used for the potentiometric and calorimetric titrations are reported in (Table 1).

The potentiometric titrations performed at different ionic strengths and at the same temperatures were analyzed altogether using the software BSTAC [21], that is able to refine the ionic strength dependence parameters inputting raw potentiometric data. This analysis, performed at the four temperatures (283.15, 298.15, 310.15 and 318.15 K), produced smoothed equilibrium constant values reported in (Table 2) and ionic strength dependence parameters.

The analysis of the data needs the knowledge of the ligand protonation constants and the metal hydrolysis constants in the same experimental conditions of the measurements. For the Ca^{2+}/Ris^{4-} system, the risedronate protonation constants were taken from Bretti, et al. 15, whereas the Ca^{2+} hydrolysis constants from Baes and Mesmer [30].

The calorimetric measurements performed at *I* = 0.15 mol dm^{-3} in the experimental conditions reported in (Table 1) allowed us to determine the enthalpy changes for all the species. The experimental values of the enthalpy changes are -9 ± 1, 12 ± 5, -28 ± 3 and -10 ± 4 kJ mol^{-1} for the CaL^{2-}, Ca_2L, $CaHL^{-}$ and CaH_2L (according to eq. (1)), respectively. The data analysis of the equilibrium constants at different temperatures and ionic strengths was performed together with the complex formation enthalpy changes, fitting all the data to eq. (9), in order to determine all the ionic strength and temperature dependence parameters, that are reported in (Table 3).

The data in (Table 3) are useful to determine the equilibrium constants of the Ca^{2+}/Ris^{4-} species at any value of temperature and ionic strength within the experimental range used for the measurements. This gives the possibility to predict the speciation of risedronate in the conditions of natural fluids, if all the network of interactions among the different components of the fluid is known.

Case Report

In this work, three natural fluids were chosen, saliva, human blood plasma and urine. The choice was driven by the fact that risedronate may be present in all these three media: in the first two, saliva and blood plasma, because it is administered as tablets or by intravenous injection and in the third, urine, because it is excreted by this system. First of all, the composition of the fluids has been taken from the most

Table 2: Smoothed complex formation constant values of the Ca^{2+}/Ris^{4-} system (according to eq. (1)) and risedronate protonation constants (according to eq. (2)) taken from Bretti, et al. [15]

I [a]	T [b]	CaL	Ca_2L	CaHL	CaH_2L	HL	H_2L	H_3L	H_4L
0.15	283.15	6.15±0.07 [c]	8.75±0.23 [c]	3.44±0.07 [c]	2.85±0.08 [c]	10.872	17.857	23.910	26.063
0.50	283.15	5.42±0.06	7.51±0.16	3.01±0.06	2.60±0.07	10.534	17.316	23.209	25.305
1.00	283.15	5.04±0.06	6.74±0.37	2.89±0.07	2.58±0.07	10.381	17.121	22.951	25.049
3.00	283.15	4.68±0.13	5.41±1.53	3.28±0.19	3.06±0.12	10.351	17.358	23.223	25.475
0.15	298.15	6.09±0.04	8.86±0.23	3.18±0.05	2.83±0.07	10.940	17.748	23.534	25.685
0.50	298.15	5.36±0.04	7.59±0.16	2.74±0.05	2.58±0.06	10.537	17.133	22.780	24.857
1.00	298.15	4.98±0.04	6.80±0.37	2.62±0.06	2.56±0.06	10.303	16.851	22.468	24.524
3.00	298.15	4.67±0.10	5.44±1.53	3.05±0.16	3.07±0.10	9.961	16.764	22.561	24.682
0.15	310.15	6.05±0.06	8.94±0.23	2.98±0.08	2.82±0.04	10.990	17.670	23.260	25.410
0.50	310.15	5.30±0.06	7.65±0.16	2.54±0.08	2.57±0.06	10.540	17.000	22.470	24.530
1.00	310.15	4.91±0.09	6.85±0.37	2.42±0.09	2.55±0.06	10.250	16.650	22.120	24.140
3.00	310.15	4.59±0.12	5.46±1.53	2.88±0.15	3.07±0.09	9.680	16.330	22.080	24.100
0.15	318.15	6.03±0.09	8.99±0.23	2.86±0.09	2.81±0.05	11.020	17.618	23.088	25.237
0.50	318.15	5.28±0.08	7.69±0.16	2.41±0.09	2.56±0.04	10.542	16.917	22.271	24.325
1.00	318.15	4.91±0.08	6.88±0.37	2.30±0.08	2.54±0.04	10.210	16.530	21.895	23.901
3.00	318.15	4.67±0.16	5.48±1.53	2.77±0.17	3.08±0.10	9.498	16.059	21.775	23.741

[a] in mol dm^{-3}; [b] in K; [c] 95% C.I. (Confidence Interval).

Table 3: Ionic strength and temperature dependence parameters of eq. (9) for the Ca^{2+}/Ris^{4-} system, at infinite dilution.

Species [a]	log K_{ij}^0	z^*	C_{ij}	ΔH_{ij0}^0 [b]	$C_{ij}^{'}$
$CaLH_2$	3.77±0.03 [c]	8	0.42±0.03 [c]	0.82±2.2 [c]	2.0±0.3 [c]
$CaLH^-$	4.61±0.04	12	0.46±0.03	-25.0±2.7	2.9±0.4
CaL^{2-}	8.07±0.04	16	0.18±0.02	-0.5±2.0	3.9±0.5
Ca_2L	11.9±0.3	24	-0.2±0.5	21±5	

[a] according to eq. (1); [b] in kJ mol^{-1}; [c] ± 95% C.I.

reliable reference books, even if the composition depends on several factors like, e.g., age, sex, particular conditions and/or pathologies, kind of organism. A table with the composition of the fluids is given in (Table 4).

As a second step, the stability constants of all the species formed among the components reported in (Table 4) must be determined. The stability constants database [33-36] and other reference papers were used for this purpose [32-35,37-39]. Together with these species, those formed by drug and the components must be known, and in this case between Mg^{2+} and Ca^{2+} with risedronate. Data of the Ca^{2+}/Ris^{4-} system are here reported, those of Mg^{2+}/Ris^{4-} are reported elsewhere [40].

All the equilibrium constants calculated for the case studies are reported as supplementary material.

The case studies were built considering [41] species for urine, and 106 for both human blood plasma and saliva. In all cases, the concentration of risedronate considered is 0.005 mol dm^{-3}. This value was decided taking into account that the amount of a tablet of risedronate dissolved in a volume of 50-100 cm^3.

The speciation of risedronate in urine is reported in (Figure 2) in the pH range 5-7. The most important protonated species is the $H_3(Ris)^-$ at pH ~ 5.0 (0.5 molar fraction), the $H_2(Ris)^{2-}$ at pH ~ 6.0 (0.3 molar fraction), and the monoprotonated at pH ~ 7.0 (0.3 molar fraction). Complex species with Ca^{2+} are formed in important amounts, namely 0.25 molar fraction of the neutral $CaH_2(Ris)$ at pH ~ 6.0 and 0.2 molar fraction of $CaH(Ris)^-$ at pH ~ 7.0. The corresponding Mg^{2+} species are formed in the same pH range, but the formation percentages are halved with respect to the Ca^{2+} ones.

Table 4: Composition of the case studies considered in this work in terms of concentration of ions (in mol dm^{-3}).

	Blood Plasma	Urine	Saliva
	[31]	[a]	[32]
pH	7.4	6.1	6.5
I / mol dm^{-3}	0.1506	0.3035	0.1063
Chloride	0.10370	0.09040	0.02530
Carbonate	0.02490		0.01145
Sulphate	0.00049	0.00967	0.00110
Fluoride	0.00001		0.00003
Phosphate	0.00160	0.03640	0.00850
Sodium	0.14260	0.09460	0.02030
Potassium	0.00406	0.02860	0.02890
Calcium	0.00244	0.00263	0.00210
Magnesium	0.00078	0.00179	0.00050
Glutathione	0.00109		
Citrate	0.00009	0.00148	
Monocarboxylates	0.00105		
Dicarboxylates	0.00029	0.00023	
Thiocyanate	0.00002		0.00020
Amino Acids	0.00308		0.00035
Fat Acids	0.01300		
Urea	0.00453	0.19200	0.00033
Ammonia	0.00003	0.01640	0.00035
Mono amines		0.00119	

[a] from a group of 2872 people (unpublished data from this laboratory).

Table 5: Formation percentages of Mg^{2+} and Ca^{2+} species in Urine in the presence of risedronate (c_L = 5 mmol dm^{-3}) at pH = 6.5.

Species	M = Mg^{2+}	M = Ca^{2+}
Free M^{2+}	27.61	27.48
M(Urea)	4.85	1.53
M(Cit)$^-$	6.83	10.77
MSO_4	24.98	21.67
$MHPO_4$	10.17	7.34
$MH_2PO_4^+$	3.14	2.32
M(Ris)$^{2-}$	0.82	0.65
M_2(Ris)	1.40	0.40
MH(Ris)$^-$	12.69	13.85
MgH_2(Ris)	6.07	13.53
Minor species [a]	1.42	0.41
Total	100.0	100.0
Sum of M^{2+}/Ris^{4-} species	**20.98**	**28.43**

[a] Sum of species with less than 1%.

Table 6: Formation percentages of Mg^{2+} and Ca^{2+} species in Saliva in the presence of risedronate (c_L = 5 mmol dm^{-3}) at pH = 7.0.

Species	M = Mg^{2+}	M = Ca^{2+}
free M^{2+}	16.11	17.81
$MHCO_3^+$	0.76	1.37
$MHPO_4$	8.60	6.89
$MH_2PO_4^+$	0.81	0.67
M(Ris)$^{2-}$	5.14	16.39
MH(Ris)$^-$	57.02	46.73
MH_2(Ris)	7.60	5.07
M_2(Ris)	1.31	1.94
Minor species [a]	2.60	3.10
Tot	100.0	100.0
Sum of M^{2+}/Ris^{4-} species	**71.07**	**70.12**

[a] Sum of species with less than 1%.

The distribution of Ca^{2+} and Mg^{2+} in urine in the presence of risedronate is described in (Table 5), there it can be observed that the summation of the Ca^{2+}/Ris^{4-} species reach a total of 28% and that of the Mg^{2+}/Ris^{4-} ones 21%. When only the "natural" components are present, at pH ~ 6.5 Mg^{2+} as free cation (37%), $MgCit^-$ (35%), $MgHPO_4$ (24%), $MgSO_4$ (4%) and Ca^{2+} is present as free cation (49%), CaHPO4 (31%), $CaCit^-$ (12%), and $CaSO_4$ (7%) and minor species (1%) [41].

In the case of saliva at the same concentration of risedronate, the chemical distribution of its species is depicted in (Figure 3). The pH of formation of the molar fraction of each species is very similar to what observed in the case of urine, except for the lower formation percentages of the Mg^{2+} species that depends on the lower concentration of this cation in saliva than urine. Normally, in this medium, at pH = 7.0, Ca^{2+} is present as free cation (65%), $CaHPO_4$ (27%), $CaHCO_3^+$ (5%) and $CaH_2PO_4^+$ (3%) and, similarly, Mg^{2+} is distributed among: free cation (45%), $MgHPO_4$ (33%), $MgSO_4$ (4%) and $MgHCO_3^+$ (3%). If risedronate is also considered, the speciation of Mg^{2+} and Ca^{2+} is very different, in fact looking at (Table 6), we may observe that more than 70% of both alkaline earth metal cations are complexed by risedronate.

In blood plasma, the speciation of Ca^{2+} and Mg^{2+} was studied by May, et al. [39] reporting that, at pH = 7.4, more or less 45 % of total Ca^{2+} is bound to protein and it is not exchangeable with low molecular weight ligands, whereas the rest is distributed as follows: Ca^{2+} (34%), $CaHCO_3^+$ (9%), $Ca(Cit)^-$ (4%), $Ca(Lact)^+$ (3%), $CaPO_4^-$ (3%) and $CaCO_3$ (2%). Considering the presence of risedronate (c_L = 5 mmol dm^{-3}) the distribution is dramatically modified, in fact as depicted in (Figure 4), 45% of Ca^{2+} is bound to proteins, but 36% is bound to various risedronate species and only 10% is free. As regards the speciation of risedronate, 57% is protonated (48% as H(Ris) and 9% as H_2(Ris)), 32% is present as Ca^{2+}/Ris^{4-} species and 11% as Mg^{2+}/Ris^{4-} species.

Conclusion

In this work, the complexing ability and the thermodynamic of binding for the Ca^{2+}/Ris^{4-} system is analyzed by means of

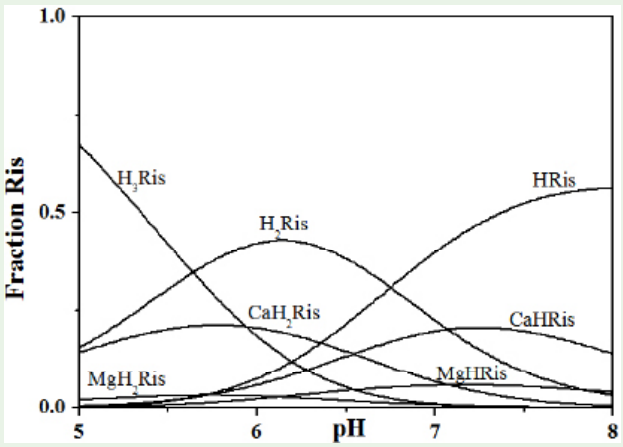

Figure 3: Speciation of risedronate in saliva at T = 310.15 K and I = 0.1063 mol dm^{-3}.

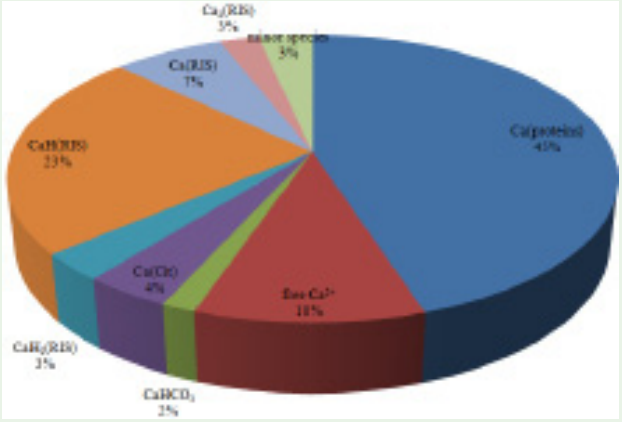

Figure 4: Distribution of Ca^{2+} species in human blood plasma at T = 310.15 K and I = 0.1506 mol dm^{-3}.

potentiometric and calorimetric measurements. Four species were determined, namely CaL, Ca_2L, CaHL and CaH_2L. Using proper equations as Debye-Hückel, SIT and Clarke and Glew, it was possible to compute the equilibrium constants of these species in the conditions of some important natural fluids, together with the equilibrium constants of all the components of human blood plasma, urine and salive. Inputting the analytical concentration of each component and the values of each equilibrium constants, computer simulation softwares such as Hyss was able to predict the chemical speciation of any of the component of interest. In this work, it was found that in urine, the presence of risedronate affects significantly the speciation of alkaline earth metal cations, achieving a total of 21 and 28% of formation of Mg^{2+}/Ris^{4-} and Ca^{2+}/Ris^{4-} species, respectively. In this medium, however, the contribution of hydroxyapatite is missing. In blood plasma, the complexation of risedronate is even more efficient, yielding a total of 36% of Ca^{2+}/Ris^{4-} species. Even if the total concentration of Ca^{2+} in both media is similar, the pH of plasma is more than one order of magnitude higher than that of urine, therefore risedronate is more deprotonated and available for complexation with metal cations. In this medium, the contribution of proteins is hard to be modelled and their contribution is fixed to 45% of total Ca^{2+}, as suggested by May, et al. [39]. The most interesting results were obtained for saliva, where more than 70% of both Ca^{2+} and Mg^{2+} are present as a complex with risedronate, probably because this is the most diluted fluid and, consequently, the competition of other ligands (such as citrate, phosphate etc...) for the binding of metal cations is scarce. Considering these data, the scarce absorption of risedronate in the presence of water with high levels of Ca^{2+} and Mg^{2+} may be better understood.

It must be remarked that the results obtained in this work are valid for the concentration of risedronate considered, but they could be used to find the best way for the administration of risedronate.

One of the aims of future studies will be the quantification of the interaction between risedronate and hydroxyapatite and how to find the way to consider this interaction into this model. Errassifi, et al. [8] studied these interactions, concluding that the adsorption of risedronate on apatitic support corresponds to an ion substitution reaction with phosphate anions at the crystal surface. Even if this mechanism is the object a lively scientific debate, the question on how to take into account this contribution in solution equilibria remains unresolved.

This work underlines very well how important can be the determination of equilibrium constant and enthalpy changes of interaction, because they give the possibility to predict the fate of a drug in a complex system as natural fluids.

References

1. Prasad C, Greenspan SL, Vujevich KT, Brufsky A, Lembersky BC, Van Londen GJ, et al. Risedronate may preserve bone micro architecture in breast cancer survivors on aromatase inhibitors: A randomized, controlled clinical trial. Bone. 2016; 90: 123-126.
2. Fleisch H A, Bisphosphonates. Preclinical Aspects and Use in Osteoporosis. Annals of Medicine. 1997; 29: 55-62.
3. Lloyd SA, Morony SE, Ferguson VL, Simske SJ, Stodieck LS, Warmington. Osteoprotegerin is an effective countermeasure for spaceflight-induced bone loss in mice. Bone. 2015; 81: 562-572.
4. Chou ACC, Ng ACM, Png MA, Chua DTC, Ng DCE, Howe TS, et al. Bone cross-sectional geometry is not associated with atypical femoral fractures in Asian female chronic bisphosphonate users. Bone. 2015; 79: 170-175.
5. Hofstetter B, Gamsjaege S, Phipps RJ, Recker RR, Ebetino FH, Klaushofer K, et al. Effects of alendronate and risedronate on bone material properties in actively forming trabecular bone surfaces. Journal of Bone and Mineral Research. 2012; 27: 995-1003.
6. Tassone P, Tagliaferri P, Viscomi C, Palmieri C, Caraglia M, D'Alessandro A, et al. Zoledronic acid induces antiproliferative and apoptotic effects in human pancreatic cancer cells in vitro. Br J Cancer 2003; 88: 1971-1978.
7. Malavasi M, Louro R, Barros MB, Teixeira LN, Peruzzo DC, Joly JC, et al. Effects of risedronate on osteoblastic cell cultures. Archives of Oral Biology. 2016; 68: 43-47.
8. Errassifi F, Sarda S, Barroug A, Legrouri A, Sfihi H, Rey C. Infrared, Raman and NMR investigations of risedronate adsorption on nanocrystalline apatites. Journal of Colloid and Interface Science. 2014; 420: 101-111.
9. Mukherjee S, Huang C, Guerra F, Wang K, Oldfield E. Thermodynamics of Bisphosphonates Binding to Human Bone: A Two-Site Model. J Am Chem Soc. 2009; 131: 8374-8375.
10. Ironside MS, Duer MJ, Reid DG, Byard S. Bisphosphonate protonation states, conformations, and dynamics on bone mineral probed by solid-state NMR without isotope enrichment. Eur J Pharm Biopharm. 2010; 76: 120-126.
11. Deacon GB, Forsyth CM, Greenhill NB, Junk PC, Wang J. Coordination Polymers of Increasing Complexity Derived from Alkali Metal Cations and (4-Amino-1-hydroxybutylidine)-1,1-bisphosphonic Acid (Alendronic Acid): The Competitive Influences of Coordination and Supramolecular Interactions. Crystal Growth & Design. 2015; 15: 4646-4662.
12. Itoh A, Akagi Y, Shimomura H, Aoyama T. Interaction between Bisphosphonates and Mineral Water: Study of Oral Risedronate Absorption in Rats. Biological and Pharmaceutical Bulletin. 2016; 39: 323-328.
13. Matczak-Jon E, Videnova-Adrabińska V. Supramolecular chemistry and complexation abilities of diphosphonic acids. Coord Chem Rev. 2005; 249: 2458-2488.
14. Foti C, Giuffrè O, Sammartano S. Thermodynamics of HEDPA protonation in different media and complex formation with Mg2+ and Ca2+. J Chem Thermodyn. 2013; 66: 151-160.
15. Bretti C, Cukrowski I, De Stefano C, Lando G. Solubility, Activity Coefficients and Protonation Sequence of Risedronic Acid. J Chem Eng Data. 2014; 59: 3728-3740.
16. Bretti C, Cigala RM, Crea F, Lando G, Sammartano S. Thermodynamics of proton binding and weak (Cl-, Na+ and K+) species formation, and activity coefficients of 1,2-dimethyl-3-hydroxypyridin-4-one (deferiprone). J Chem Thermodyn. 2014; 77: 98-106.
17. Bretti C, De Stefano C, Lando G, Sammartano S. Thermodynamic properties of melamine (2,4,6-triamino-1,3,5-triazine) in aqueous solution. Effect of ionic medium, ionic strength and temperature on the solubility and acid–base properties. Fluid Phase Equilibr. 2013; 355: 104-113.
18. De Stefano C, Gianguzza A, Pettignano A, Sammartano S, Sciarrino S. On the Complexation of Cu(II) and Cd(II) With Polycarboxyl Ligands. Potentiometric Studies With ISE-H+, ISE-Cu2+, and ISE-Cd2+. J Chem Eng. Data. 2010; 55: 714–722.
19. Sgarlata C, Zito V, Arena G. Conditions for calibration of an isothermal titration calorimeter using chemical reactions. Anal Bioanal Chem. 2012; 405: 1085-1094.
20. De Stefano C, Princi P, Rigano C, Sammartano S. Computer Analysis of Equilibrium Data in Solution. ESAB2M: An Improved Version of the ESAB Program. Ann Chim (Rome). 1987; 77: 643-675.
21. De Stefano C, Sammartano S, Mineo P, Rigano C. Computer Tools for the Speciation of Natural Fluids. In Marine Chemistry - An Environmental Analytical Chemistry Approach. Gianguzza A, Pelizzetti E, Sammartano S. Eds. Kluwer Academic Publishers: Amsterdam. 1997; 71-83.

22. Alderighi L, Gans P, Ienco A, Peters D, Sabatini A, Vacca A. Hyperquad Simulation and Speciation (HySS): a utility program for the investigation of equilibria involving soluble and partially soluble species. Coord Chem Rev. 1999; 194: 311-318.

23. De Stefano C, Foti C, Sammartano S, Gianguzza A, Rigano C. Equilibrium studies in natural fluids. Use of synthetic seawater and other media as background salts. Ann Chim (Rome). 1994; 84: 159-175.

24. Brönsted JN. Studies on solubility IV. Principle of the specific interaction of ions. J Am Chem Soc. 1922; 44: 887-898.

25. Ciavatta L. The specific interaction theory in the evaluating ionic equilibria. Ann Chim (Rome). 1980; 70: 551-562.

26. Grenthe I, Puigdomenech I. Modelling in aquatic chemistry. OECD-NEA: Paris, France. 1997.

27. Guggenheim EA, Turgeon JC. Specific interaction of ions. Trans Faraday Soc. 1955; 51: 747-761.

28. Scatchard G. Concentated solutions of strong electrolytes. Chem Rev. 1936; 19: 309-327.

29. Setschenow JZ. Uber Die Konstitution Der Salzlosungenauf Grund Ihres Verhaltens Zu Kohlensaure. Z Physik Chem. 1889; 4: 117-125.

30. Baes CF, Mesmer RE. The Hydrolysis of cations. Wiley: New York. 1976.

31. Lentner C. Geigy Scientific Tables, 8th ed. CIBA-Geigy: Basilea, Switzerland. 1983.

32. Crea F, De Stefano C, Milea D, Pettignano A, Sammartano S. SALMO and S_3M: A Saliva Model and a Single Saliva Salt Model for Equilibrium Studies. Bioinorg Chem Appl. 2015; 2015: 12.

33. Martell AE, Smith RM, Motekaitis RJ. NIST Standard Reference Database 46, vers.8. Gaithersburg. 2004.

34. May PM, Muray K. Jess, a joint expert speciation system-II. The thermodynamic database. Talanta. 1991; 38: 1419-1426.

35. Pettit D, Powell K. IUPAC Stability Constants Database. Academic Software: Otley, UK. 2004.

36. Sillén LG, Martell AE. Stability Constants of Metal Ion Complexes. Special Publ. 17. The Chemical Society, Wiley: London. 1964.

37. Daniele PG, De Stefano C, Marangella M, Rigano C, Sammartano S. URSUS: A Computer Program for Urine Speciation. Biochim Clin. 1989; 13: 507-510.

38. Marangella M, Petrarulo M, Vitale C, Daniele PG, Sammartano S, Coseddu D, et al. Serum Calcium Oxalate Saturation in Patients on Manteinance Haemodialysis for Primary Hyperoxaluria or Oxalois-unrelated Renal Diseases. Clin Sci. 1991; 81: 483-490.

39. May PM. Linder PW, Williams DR. Computer simulation of metal-ion equilibria in biofluids: models for the low-molecular-weight complex distribution of calcium(II), magnesium(II), manganese(II), iron(III), copper(II), zinc(II), and lead(II) ions in human blood plasma. J Chem Soc Dalton Trans. 1977; 588-595.

40. Bretti C, De Stefano C, Lando G, Majlesi K, Sammartano S. Thermodynamics (Solubility and Protonation Constants) of Risedronic Acid in Different Media and Temperatures (283.15 K to 318.15 K). J Solut Chem. submitted.

41. Bretti C, Cigala RM, De Stefano C, Lando G, Sammartano S. Understanding the bioavailability and sequestration of different metal cations in the presence of a biodegradable chelant S,S-EDDS in biological fluids and natural waters. Chemosphere. 2016; 150: 341-356.